UNIVERSITÀ
DEGLI STUDI
FIRENZE

DOTTORATO DI RICERCA IN

FARMACOLOGIA, TOSSICOLOGIA E TRATTAMENTI INNOVATIVI

CICLO XXVII

COORDINATORE PROF.SSA ELISABETTA TEODORI

MT2, a NGF-mimetic compound, decreases myocardial damage induced by ischemia / reperfusion injury

Settore Scientifico Disciplinare BIO/14

Dottorando
Dott. Giuseppe Castronovo

Tutore Teorico
Prof. Federico Cozzolino

Tutore Scientifico
Prof. Domenico Edoardo Pellegrini-Giampietro

Coordinatore
Prof.ssa Elisabetta Teodori

Anni 2012/2014

INDEX

I. BACKGROUND

Ischemic heart disease (IHD) is the leading cause of death and disability in the world with over 1.9 million and 600,000 deaths per years, in the Europe and the United States, respectively. The major clinical manifestation of ischemic heart disease is usually attributable to the detrimental effects of ischemia/reperfusion (I/R) injury which leads to myocardial injury, cardiomyocyte death and cardiac dysfunction[1].

Ischemia and reperfusion is a pathological condition characterized by an initial restriction of blood supply to an organ followed by the subsequent restoration of perfusion and concomitant reoxygenation. After an acute myocardial infarction, early and successful myocardial reperfusion with the use of thrombolytic therapy or primary percutaneous coronary intervention (PCI) is the most effective strategy for reducing the size of a myocardial infarct and improving the clinical outcome. Perhaps surprisingly, although essential to salvage viable myocardium, the process of reperfusion can in itself induce myocardial injury and cardiomyocyte death, a process which has been called "myocardial reperfusion injury"[2]. Apart from limiting acute myocardial ischemic injury by timely reperfusion, there is currently no effective therapeutic intervention for protecting the heart against acute I/R injury, and therefore, novel cardioprotective therapies are still required to improve clinical outcomes in patients with ischemic heart disease[3].

The process of reperfusion injury was first postulated in 1960 by Jennings *et al.*[4] as significant morphological alterations appearing after the onset of reperfusion, including cell swelling, contracture of myofibrils, disruption of the sarcolemma, and the appearance of intra-mitochondrial calcium phosphate particles.

Studies in animal models suggest that reperfusion injury is responsible for more than 50% of the final extension of the infarcted area because the reflow of blood to ischemic myocardial tissue triggers necrosis and apoptosis in the myocytes[5].

The importance of apoptosis in cell death following reperfusion has been demonstrated in *in vivo* rodent models, allowing also the evaluation of pharmacological, growth factor mediated and genetic[6]. Many strategies to reduce reperfusion damages and reperfusion-induced apoptosis were successful in experimental models of I/R injury; however the results in clinical trials have been quite disappointing[7;8].

I.1. Ischemia and reperfusion injury

I.1.1. Molecular mechanism of cellular damage

During ischemia, a limited supply of oxygen and metabolic substrates results in a series of abrupt biochemical and metabolic changes within the myocardium (figure 1). The absence of oxygen halts oxidative phosphorylation, leading to mitochondrial membrane depolarization, ATP depletion and inhibition of myocardial contractile function. In this condition cellular metabolism switches to anaerobic glycolysis, resulting in the accumulation of lactate which reduces intracellular pH (to <7.0).

Since myocytes are trying to correct the load of acidosis by extruding H^+ ions through the Na^+/H^+ exchanger, then this induces the accumulation of Na^+, which in turn can not be removed from the cytosol through the Na^+/K^+-ATP pumps because of the lack of ATP itself. The subsequent activation of Na^+/Ca^{2+} exchanger in reversed mode helps to exchange Na^+ with the extracellular environment but developments intracellular Ca^{2+} overload[9]. All these changes, combined with the accumulation of toxic catabolites, oxygen free radicals and reduced pH, have important effects on membrane potential, contractility and cell activation status of several Ca^{2+} dependent protease. All these events associated with the ongoing ischemia are able to induce cell death[10].

The end of ischemia is marked by the beginning of reperfusion that appears to exacerbate the impact of pathological process induced by ischemia[11-13]. Thus it is probable that ischemic injury and reperfusion injury are two facets of the same problem, in which ischemic injury is associated with alterations in myocardial metabolism, including depletion of energy stores, and the reperfusion injury is associated with additional changes, including the development of oxidative stress and the occurrence of intracellular Ca^{2+} overload.

I.2. Cardiac dysfunction induced by myocardial reperfusion

The injury to the heart during myocardial reperfusion causes four types of cardiac dysfunction.

The first type is myocardial stunning, that is referred to reversible post-ischemic contractile dysfunction that occurs on reperfusing acute ischemic myocardium and it is caused by from the detrimental effects of oxidative stress and intracellular calcium overload on the myocardial contractile apparatus[14]. The myocardium usually recovers from this reversible form of injury after several days or weeks.

The second type of cardiac dysfunction, the no-reflow phenomenon was first described by Krug *et al*. in 1966 as the "inability to reperfuse a previously ischemic region"[15]. It refers to the impedance of microvascular blood flow encountered during opening of the infarct-related coronary artery and the major contributing factors include capillary damage with impaired vasodilatation, external capillary compression by endothelial cell and cardiomyocyte swelling, micro-embolization of friable material released from the atherosclerotic plaque, platelet micro-thrombi, the release of soluble vasomotor and thrombogenic substances, and neutrophil[16;17].

The third type of cardiac dysfunction, reperfusion arrhythmias, is caused by the sudden reperfusion of acutely ischemic myocardium. This event is potentially harmful, however effective treatments are available[18].

Finally, reperfusion-induced death of cardiomyocytes that were viable at the end of the index ischemic event is defined as lethal myocardial reperfusion injury[19]. The major contributory factors include hypercontracture, oxidative stress, mitochondrial permeability transition pore (MPTP) opening, and calcium overload. The existence of lethal myocardial reperfusion injury has been inferred in both experimental myocardial infarction models and in patients with myocardial infarction and may account for up to 50% of the final myocardial infarction size, for this reason it represents an important target for cardioprotection in primary percutaneous coronary intervention patients[2].

Nevertheless, no effective therapy currently exists for reducing lethal myocardial reperfusion injury in patients who have undergone primary percutaneous coronary intervention.

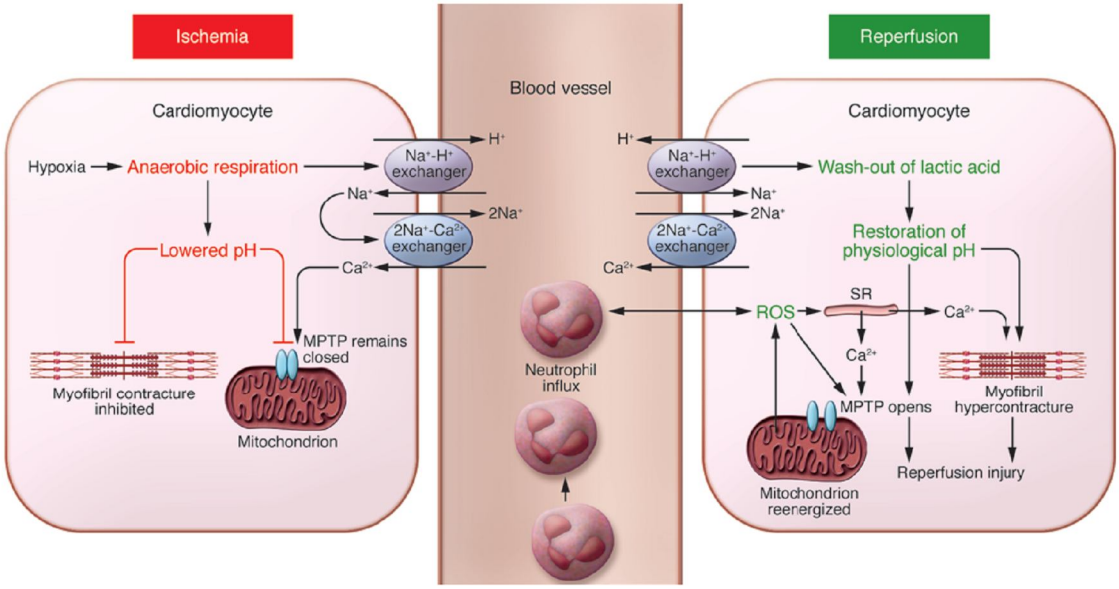

Figure 1: Schematic illustrating the main proponents of acute myocardial I/R injury[3].

I.2.1. The hypercontracture

The first pathological feature related to I/R was the hypercontracture of myocytes with the formation of contraction bands along the reperfused myocardium.

The ultimate mechanism of hypercontraction during reperfusion has not been fully elucidated, but ample evidence suggests that the cytosolic Ca^{2+} overload plays a critical role. Accumulation of intracellular Na^{+} and Ca^{2+} during ischemia occurs in response to the loss of energy homeostasis and as a result of changes in the acute regulation of sarcolemmal and sarcoplasmic reticulum cation transport mechanisms. Specifically, ischemia reduces the activity of sarcolemmal Na^{+}/K^{+}-ATPase, increases the activity of the Na^{+}–H^{+} exchanger, and promotes the activation of the Na^{+}–Ca^{2+} exchanger in a reverse mode.

At the time of myocardial reperfusion there is an abrupt increase in intracellular Ca^{2+} that is secondary to sarcolemmal-membrane damage and oxidative stress-induced dysfunction of the the sarcoplasmatic reticulum[20;21]. The result is intracellular and mitochondrial Ca^{2+} overload, and this excess of Ca^{2+} induces cardiomyocyte death by causing hypercontracture of the heart cells and mitochondrial permeability transition pore opening[19].

In experimental studies has been demonstrated that attenuation of Ca^{2+} overload with pharmacologic antagonists of the sarcolemmal Ca^{2+} ion channel, the mitochondrial Ca^{2+} uniporter, or the sodium–hydrogen exchanger, reduce myocardial infarction size by up to 40–60%[22;23].

However, the results of the corresponding clinical studies have been negative because an important issue in the clinical scenario is that in the animal studies the Ca^{2+} loading inhibitors were administered during ongoing ischemia while in the human trial at the beginning of reperfusion, when Ca^{2+} overload already happened[7;9;24;25].

I.2.2. Oxidative stress

In the first few minutes of myocardial reperfusion, a burst of oxidative stress is produced by a variety of sources[26;27]. In myocytes, mitochondria comprise 30–40% of the volume, and generate about 90% of the ATP. Mitochondria are also the major source of reactive oxygen species (ROS) in the cardiovascular system[28]. Free radicals are generated by one electron reduction or oxidation of molecules creating an unpaired electron.

In normal mitochondrial oxidative phosphorylation, O_2 is reduced by four electrons to form H_2O. The energy derived from this reduction of O_2 serves to meet the energy demands of the cell. Paradoxically, it is also the actual process of oxygen reduction that leads to the formation of oxygen free radicals. Incomplete reduction of O_2 leads to the generation of superoxide anion (O_2^-), hydrogen peroxide (H_2O_2), and hydroxyl radical (OH). O_2^- is unstable with a lifetime of milliseconds at neutral pH, and in aqueous solution it spontaneously reacts or dismutates to yield H_2O_2 and O_2.

During the reperfusion phase the ROS generated cause cellular calcium loading with inhibition of the sarcoplasmic reticulum calcium ATPase and inhibition of the sodium potassium ATPase leading to sodium-mediated calcium gain[29].

ROS cause also lipid peroxidation that can result in cell membrane breakdown causing cell swelling. In addition during myocardial reperfusion, oxidative stress also reduces the bioavailability of the intracellular signaling molecule, nitric oxide, thereby removing its cardioprotective effects such as inhibition of neutrophil accumulation, inactivation of superoxide radicals, and improvement of coronary blood flow[30].

Based on these observations, antioxidant therapy was naturally considered to be an appropriate option to prevent such injury. However, both experimental and clinical studies have reported mixed results with the administration of antioxidant therapy at the onset of myocardial reperfusion. The reason for this may in part be due the inability of the antioxidant to enter the cell[31].

I.2.3. The opening of MPTP

Many of the actors of myocardial reperfusion injury appear to converge on the mitochondrial permeability transition pore. The MPTP is a non selective channel of the inner mitochondrial membrane and are made by the linking of an adenine nucleotide translocase (ANT) with a voltage-dependent anionic channel (VDAC or so called "porine"). Cyclophilin D represents the regulatory portion of the pore and it is inhibited by cyclosporine.

Under normal physiological conditions, the mitochondrial inner membrane is impermeable; however, during stress condition (as myocardial reperfusion), MPTP allows free passage of any molecule of <1.5 kDa[32-34]. When the MPTP opens, the permeability barrier of the inner membrane becomes disrupted and all small molecular weight solutes move freely across the membrane exerting a colloidal osmotic pressure that causes mitochondria to swell. This condition causes rupture of the outer membrane that will lead to the release of proteins in the intermembrane space such as cytochrome *c* and other factors that play a critical role in apoptotic cell death. Moreover the inner membrane becomes freely permeable to protons causing uncoupled oxidative phosphorylation, this event leads to hydrolyse ATP, rather than synthesis it. In such conditions, intracellular ATP concentrations rapidly decline, leading to the disruption of ionic and metabolic homeostasis and the activation of degradative enzymes such as phospholipases, nucleases, and proteases. Unless pore closure occurs, these changes will cause irreversible damage to the cell, resulting in necrotic death[35]. In the setting of acute myocardial I/R injury, the MPTP has been shown to remain closed during ischemia and only open at reperfusion in response to mitochondrial Ca^{2+} and phosphate overload, oxidative stress and relative ATP depletion, and rapid pH correction[36].

As such, preventing MPTP opening at the time of reperfusion by administering known MPTP inhibitors (such as the immunosuppressant cyclosporin A) at the onset of myocardial reperfusion has been reported in experimental studies to reduce myocardial infarction size by 40%–50% in small and large animal myocardial infarction models and protect human atrial trabeculae subjected to simulated I/R injury[37-41]. Therefore, the MPTP provides an important therapeutic target for preventing lethal myocardial reperfusion injury.

I.3. Anti-apoptotic mechanism in I/R cardiomyocytes: RISK (Reperfusion Injury Salvage Kinase)

It has been demonstrated that is possible to protect reperfused myocardium by activating prosurvival kinase signaling pathways, now called the reperfusion injury salvage kinase pathway [42;43]. The RISK pathway emerged as a concept in the late 1990s with the recognition that apoptotic cell death contributed to lethal reperfusion injury, and the knowledge that there existed certain pro-survival anti-apoptotic protein kinases, such as Akt and ERK1/2 (extracellular signal regulated kinase 1/2), which when specifically activated at the time of myocardial reperfusion conferred powerful cardioprotection[42;44]. The cardioprotective potential of both Akt and ERK1/2 has been confirmed using transgenic activation of these kinases[45;46]. This cardioprotection has been attributed to inhibition of MPTP opening, improved uptake of Ca^{2+} in the sarcoplasmic reticulum and the recruitment of antiapoptotic pathways[44;47;48].

Studies previously demonstrated activation of these protein kinases Akt, ERK1/2 and JNK at the time of myocardial reperfusion in control hearts, but clearly the activation of the RISK pathway in these settings was not sufficient to confer cardioprotection, and an additional pharmacological stimulus was required to enhance the activation of the RISK pathway. Extensive preclinical evidences suggest that activation of the RISK pathway by pharmacologic agents or by mechanical interventions reduces myocardial infarct size by up to 50%[42;43;49].

In addition to ERK1/2 and Akt, the RISK pathway includes other cardioprotective reperfusion salvage kinases such as PKC (primarily the PKC-ε isoform), PKG, p70s6K, and GSK-3β. Conversely, protein kinases such as PKC-δ and rho-kinase which when

activated at the time of myocardial reperfusion are pro-injurious and counteract the cardioprotection elicited by the RISK pathway[42].

Among the harmful proteins that are activated in I/R injury is also p38 mitogen-activated protein kinase (MAPK), which is an important pro-apoptotic kinase in cardiomyocytes[50]. Evidence obtained from preclinical investigations showed that the inhibition of p38 MAPK during prolonged ischemia slows the rate of infarction/death and inhibits the production of inflammatory cytokines, such as tumor necrosis factor-α (TNFα), interleukin-1 (IL-1), and IL-8, which are known to aggravate ischemic injury[51;52].

Reperfusion can re-activate p38 MAPK, maybe in response to stimuli such as ROS and osmotic stress[50]. Although this field of research is still evolving, compelling evidence supports a causative role of p38 MAPK in myocardial injury and dysfunction following ischemia/reperfusion[50;53-55].

It is known that growth factors such as vascular endothelial growth factor (VEGF) and fibroblast growth factor (FGF) exert cardioprotection through the RISK pathway at the onset of myocardial reperfusion (figure 2). In fact, growth factor binding to its specific protein tyrosine kinase receptor in the heart has the ability to activate both the PI3K-Akt and MEK1/2-ERK1/2 signal transduction cascades of the cardioprotective RISK pathway. In this connection, the activation of the VEGF receptor is known to activate signal transduction pathways of the RISK pathway such as MEK1/2-ERK1/2-p90rsk within the cardiomyocyte and PI3K-Akt-eNOS within endothelial cells, which are known to mediate cytoprotection[56]. Thus, through these signaling cascades, VEGF would have the potential to protect cardiomyocytes from I/R injury.

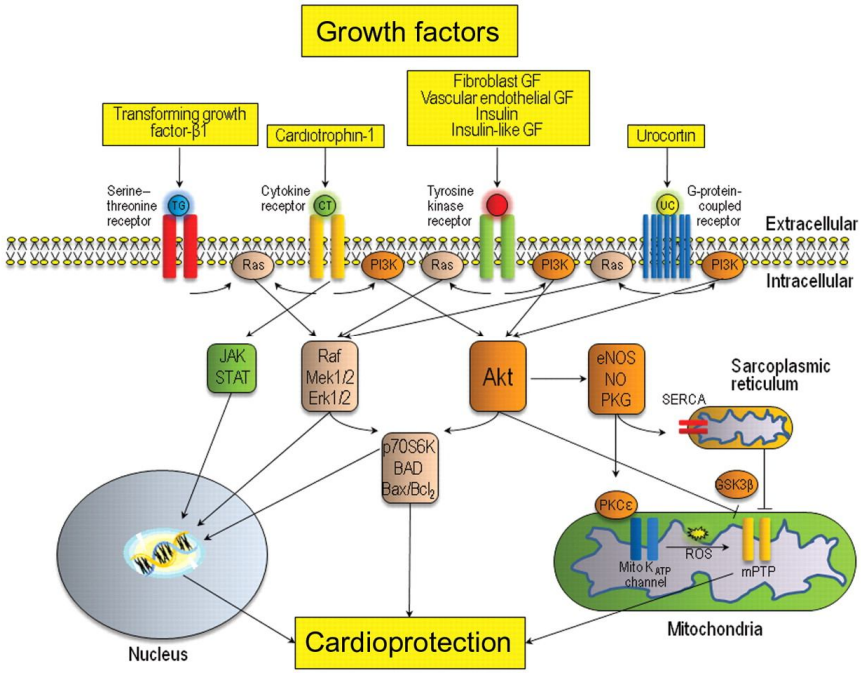

Figure 2: Intracellular transduction pathways underlying cardioprotection elicited by the growth factors[57].

I.4. Nerve Growth Factor (NGF) and myocardial ischemia

Neurotrophins are a family of growth factors that exert diverse effects on the developing and mature cardiovascular system. NGF, initially considered for its neural function was reported to be effective in maintaining the survival of cardiomyocytes following I/R events and for this reasons it can be considered a therapeutic tool for ischemic heart disease[58].

Meloni *et al.*[58] showed that NGF blockade causes apoptosis of both cardiomyocytes and endothelial cells (ECs) and this process may account for impaired myocardial functions. They demonstrated that adenovirus-mediated NGF overexpression in the mouse periinfarct myocardium stimulates angiogenesis at both capillary and arteriolar levels and reduces apoptosis of ECs and cardiomyocytes in the periinfarct myocardium through a mechanism mediated by increase of Akt and Foxo-3a phosphorylation.

This pathway was confirmed by experiments using adenovirus with a mutant form of Foxo-3a which can not be phosphorylated by Akt. In these models NGF gene therapy did not improve either myocardial angiogenesis and cardiac function[58].

In addition, local NGF gene therapy expands the number of Lineage negative c-kit positive (lin-neg c-kit-pos) cells with cardiogenic and vasculogenic capacities in the

infarcted heart by increasing the expression of the c-kit ligand stem cell factor (SCF)[58;59]. Lin-neg c-kit-pos cells are involved in myocardial repair and regeneration after myocardial infarction, and SCF induces neovascularization in the adult myocardium[59-61].

Taken together, these data provide strong evidence for the therapeutic potential of NGF in the post-myocardial infarction heart and furthermore reinforce the concept that neurotrophins have important cardiovascular actions.

II. INTRODUCTION

Neurotrophins (NTs) are a family of cytokines that regulate proliferation, differentiation, and survival of neural cells, as well as non neural cell types[62;63]. They interact with two classes of cell surface receptors: the low-affinity neurotrophin receptor p75 (p75NTR) binds all neurotrophins with similar affinity, whereas the high-affinity receptors, belonging to the superfamily of tropomyosin kinase receptor (Trk), bind each neurotrophin in a specific manner[62]: TrkA binds NGF, TrkB binds Brain Derived Neurotrophic Factor (BDNF) and NT-4/5, TrkC binds NT-3.

The overall signal imparted by neurotrophins through Trk receptors is compounded by tropic, trophic, and differentiation-inducing responses[64] and, for these reasons, neurotrophins have been proposed as therapeutic tools in many disorders, from neurodegenerative diseases to corneal neurotrophic ulcers and stroke[65].

Recent studies in experimental models of acute myocardial ischemia demonstrated the protective role of NGF in heart injury[58;66]. Unfortunately, the use of NGF as therapeutic tool in I/R injury would not be recommended due to its sensitivity to proteolysis. Peptidomimetic structures represent a useful tool in drug discovery, as modifications of bioactive peptides can result in better pharmacological properties, such as higher metabolic stability, increased bioavailability, and higher receptor affinity or selectivity[67]. In this connection, NGF mimetic compounds could provide a valid alternative strategy.

We obtained neurotrophin mimetics through the functional screening of a chemical library of compounds with spatial coordinates fitting the NGF binding site on TrkA molecule. A small number of compounds were identified based on their ability to support the survival of neural cells undergoing metabolic stress. The extensive biochemical and functional characterization of them revealed that they were endowed with NGF mimetic properties and interact with TrkA receptors. In particular, the selected compound MT2 interacts with TrkA with a K*d* of 100nM and inhibits the

apoptotic process induced by metabolic stress in neural cell cultures[68]. Huge amount of data, obtained in our laboratory, also suggest that MT2 is able to prevent the apoptotic death of several cell types (epithelial, fibroblast and myocardiocytes) induced by different pro-apoptotic stimuli.

Currently, it's largely recognized that the reperfusion process following the acute ischemia events is hallmarked by the apoptosis of cardiomyocytes and by inflammatory reaction[69]. Myocardial apoptosis begins shortly after ischemia, is strongly amplified by reperfusion, and partially contributes to the overall cardiomyocyte death[70].

We therefore evaluated the effect of MT2 in *in vitro* and *in vivo* model of myocardial ischemia. In these models we studied whether MT2 could modulate a series of events related to the reperfusion-induced apoptotic death of cardiomyocytes *in vitro* such as activation of p38 MAPK, caspase 3 and PARP activation. We also studied whether MT2 interferes in a relevant pathway which maintains the overall cell survival in I/R conditions based on VEGF function activated following ischemia-induced HIF-1 production. Moreover data obtained from *in vivo* experiments showed that MT2 treatment decreases infarcted area of about 50% compared to untreated controls.

The results obtained indicated that MT2 decreases the pathologic effects of I/R injury by interfering with both MAPK and HIF-1α/VEGF pathway, prospecting its use as therapeutic tool in acute myocardial ischemia.

III. METHODS AND MATERIALS

III.1. Cell lines and cell cultures

Rat pheochromocytoma PC12 cells were cultured in RPMI-1640 (Sigma Aldrich, St. Louis, MO, USA), supplemented with 10% horse serum, 5% fetal bovine serum (FBS). NIH-3T3 and H9C2 were cultured in DMEM supplemented with 10% FBS. All cell lines were obtained from ATCC. Culture media were supplemented with 2 mM L-glutamine and 50 IU/ml penicillin, and 50 µg/ml streptomycin.

III.2. Cell viability assay in PC12 cell line

Compounds were prepared as 10 mM stock solution using ethanol as a solvent. MTT reduction assay was carried out according to the manufacturer instructions. Briefly, cells were plated at 5×10^3 cells per well in 100 µl of serum-free medium in 96-well tissue culture plates, and treated in triplicate with 0.1–10 µM of test compounds for 3 days or with 4 nM hrNGF (Calbiochem, Darmstadt, Germany) as positive control. MTT (Sigma Aldrich) was added to a final concentration of 0.5 mg/ml, and the incubation was prolonged for further 4 h. Cells were lysed by adding 100 µl of lysis buffer (20% SDS, 50% N,N-dimethylformamide, pH 4.7) and reduced MTT was solubilized with 100 µl of isopropyl alcohol. The optical density of the resulting solution of converted dye was measured in a microplate spectrophotometer at a wavelength of 570 nm with background subtraction at 690 nm. The survival index was calculated as (MTT incorporation of stimulated cultures/background cultures) × 100.

III.3. Docking analysis of MT2 on TrkA

The docking simulations were performed on a model of TrkA ligand binding domain obtained deleting the NGF from the NGF-TrkA co-crystal (PDBcode: 1WWW). Docking was performed as a global energy optimization by means of the biased probability Monte Carlo stochastic procedure as implemented in ICM3.6 and the binding energy was assessed by the ICM empirical standard scoring function[71]. The molecular system was described using internal coordinate variables. Hydrogen atoms and missing heavy atoms were added. Zero occupancy side chains and polar hydrogen atoms were optimized and assigned the lowest energy conformations. Tautomeric states of histidines and the positions of asparagine and glutamine side chain amidic groups were optimized to improve the H-bond pattern. The ligand was assigned MMFF force field atom types, its three dimensional structure was generated from 2D coordinates, and it was subjected to Cartesian minimization. The binding site was defined selecting all the residues with at least one non-hydrogen atom within 3.5 Å from the largest envelope predicted by the Pocketome Gaussian Convolution algorithm[72]. The binding pocket was described by five 0.5 Å spacing potential grid maps, representing van der Waals potentials for hydrogens and heavy atoms, electrostatics, hydrophobicity, and hydrogen bonding. A soft form of the van der Waals potentials truncated at 4 kcal/mol was adopted.

III.4. Western blot analysis

PC12, WT or mutant TrkA NIH-3T3 cells, were stimulated for 15–30 min with 10 μM MT2 or 4 nM hrNGF as positive control. Cells were lysed with RIPA buffer (50 mM Tris-HCl, pH 7.4; 150 mM NaCl; 2 mM EDTA; 1 mM NaF; 1 mM sodium orthovanadate, 1% NP-40) in the presence of phosphatase inhibitor cocktail 2 and 3, protease inhibitor cocktail (Sigma Aldrich) and centrifuged at 12 000 r.p.m. for 15 min. Protein concentration was determined by using a Micro BCA protein assay kit (Pierce, Rockford, IL, USA). Fifty micrograms of proteins was loaded onto SDS-PAGE and blotted onto nitrocellulose filters (GE Healthcare, Fairfield, CT, USA). Membranes were stained with rabbit antibodies anti-P-TrkA-Y490, anti-P-TrkA-Y674/675, anti-P-TrkA-Y 785, anti-P-Akt, anti-P-ERK 1/2, and anti-P-SAPK/JNK (Cell Signaling Technology,

Danvers, MA, USA), anti-MKP1 (Santa Cruz Biotechnology, Santa Cruz, CA, USA), anti-VGF (OriGene, Rockville, MD, USA) and mouse anti β-actin (Santa Cruz Biotecnology); all the antibodies were used at 1:1000, final dilution. HRP-coniugated anti-rabbit IgG (GE Healthcare) or HRP-conjugated anti mouse IgG (Santa Cruz Biotecnology) were used as secondary antibodies at 1:2000 final dilution. The reactions were visualized by the ECL detection system as recommended by the manufacturer (GE Healthcare). Membranes were stripped at 65° C in stripping buffer (100 mM Mercaptoethanol, 2% SDS and 62.5 mM Tris-HCl pH 6.8) for 30 min and stained with anti-hTrkA, anti-hAkt, anti-hERK1/2, and anti-hSAPK/JNK (Cell Signaling Technology). After staining with HRP-coniugated anti-rabbit IgG, the reactions were visualized by the ECL detection system.

For the detection of proteins in *in vitro* model of ischemia/reperfusion, H9C2 cells were differentiated in cardiac muscle cells with 1% Horse Serum (HS) + 10 nM of Retinoic Acid added daily for 6 days. H9C2 cells were incubated in deep hypoxia (~0.1% O_2) for 1 hour in PBS (supplemented with Ca^{2+}/Mg^{2+}) then cells were incubated in normoxia with fresh medium (DMEM high glucose + 1% HS, 1% L-Glut, 1% P/S) with or without 10 µM MT2 for 1 or 24 hours. Cells were lysed and 30 µg of proteins were separated on 4–12% Bis-Tris SDS-PAGE gels or 4–20% Tris-Gly gels (Invitrogen, Carlsbad, CA, USA), blotted onto PVDF membranes (Millipore) and incubated overnight with the appropriate primary antibody. The antibodies used were: rabbit anti-PARP, rabbit anti-caspase 3, rabbit anti-phospho-p38 and mouse anti-total-p38, rabbit anti-phospho-ERK1/2 and mouse anti-total-ERK1/2, mouse anti-HIF-1α, mouse anti-VEGF A, rabbit anti-GAPDH.

III.5. TrkA autophosphorylation

PC12 cells and TrkA-NIH-3T3 cells were equilibrated in serum-free medium for 2 h. 5×10^6 cells were then stimulated with 10 µM of selected compounds or with 4 nM hrNGF as positive control for 15 min. Cells were then lysed with 10 mM HEPES, 142.5 mM KCl, 5 mM $MgCl_2$, 1 mM EGTA, 50 µg/ml leupeptin, 30 µg/ml aprotinin, 1 mM PMSF, 0.25% Triton X-100. Protein concentration was evaluated by Bradford assay. Two hundred fifty micrograms of cell lysates was precleared with Protein A sepha-

rose (GE Healthcare), immunoprecipitated with 2 µg/ml of rabbit a-TrkA antibodies (Genzyme, Cambridge, MA, USA) or with 2 µg of control rabbit IgG and Protein A Sepharose, eluted in Laemmli sample buffer, loaded on 10% SDS-PAGE and blotted onto nitrocellulose filters. Trk-autophosphorylation was evidenced by using rabbit anti-P-Tyr (PY350) (Santa Cruz Biotechnology). Membranes were stripped in stripping buffer at 65° C and stained with mouse anti-hTrk-A (Santa Cruz Biotechnology).
Alternatively, PC12 cells or TrkA-NIH-3T3, cultured as above, were lysed in RIPA buffer in the presence of phosphatase inhibitor cocktail 2 and 3, and protease inhibitor cocktail, and then blotted onto nitrocellulose filters (see above). Western blot analysis was performed by using rabbit anti-P-TrkA-Y490, P-Y674/675 and P-Y785 antibodies (Cell Signaling Technology).

III.6. MT2 radiolabeling

In all, 4.14 mCi of [^{3}H]MeNs solution (0.053 µmol) were concentrated under nitrogen flow and 30 µl of 0.53 µmol MT2 sodium salt in DMSO were added. The mixture was heated at 40°C for 5 min, diluted 1:2 with H_2O and loaded over a filter pre-equilibrated with 100% EtOH (5 ml) and water (12 ml). After washing with 25% EtOH in water labeled MT2 was extracted through 100% ethanol, concentrated under nitrogen flow, filtered on silica gel, washed with AcOEt (2×1 ml), again concentrated under nitrogen flow and resuspended with 100% EtOH. Specific activity was determined as the ratio between total and eluted radioactivity. Mean specific activity of ^{3}H-MT2 was 21.5 µCi/nmole.

III.7. Binding assays

III.7.1. Displacement of ^{125}I-hrNGF by MT2

PC12 cells were seeded onto 24-well plates and equilibrated with HKR medium (10 mM HEPES, 125 mM NaCl, 4.8 mM KCl, 1.3 mM $CaCl_2$, 1.2 mM $MgSO_4$, 1.2 mM KH_2PO_4, 1 g/l glucose, 1 g/l BSA). Cells were incubated in triplicate for 2 h at 4°C in

HKR medium with 0.1 nM ^{125}I-NGF in the presence or absence of different concentrations of MT2 (100–0.05 µM) of hrNGF (0.01–10 nM). Cells were washed with PBS and lysed with 0.25 N NaOH, 0.1% SDS. Unbound radioactivity and specific cell bound radioactivity were recorded by a γ-counter and data were analyzed by using the ORIGIN software (OriginLab Corporation, Northampton, MA, USA) (dose–response curve).

III.7.2. MT2 radioligand binding studies on cells

TrkA or mock transfected NIH-3T3 cells were plated at 2×10^5 cells/well in 24-well plate for 24 h, washed and equilibrated in HKR binding medium for 30 min at 4°C. Cells were then incubated with 10–0.01 µM of ^{3}H-MT2, specific activity 21.5 µCi/nmole, in the presence or absence of 100-fold excess unlabeled MT2 or 4 nM hrNGF for 2 h at 4°C. Cells were washed, lysed with 0.25 N NaOH, 0.1% SDS and, unbound and specific cell-bound radioactivity were recorded through liquid scintillation counting. Data were analyzed by the ORIGIN software (one site binding).

III.7.3. MT2 radioligand internalization studies

2×10^5 TrkA-NIH-3T3 cells were incubated in triplicate in 24-well plates with 100 nM ^{3}H-MT2, in the presence or absence of 100-fold excess MT2 or 4 nM hrNGF for 30 min at 4°C. After washing, cells were cultured at 37° C for 1 h. Membrane bound radioactivity was eluted by 0.1 M glycin buffer, pH 2, and cells were lysed with 0.25 N NaOH, 0.1% SDS. Internalized radioactivity was measured through liquid scintillation counting. 2×10^7 red blood cells were incubated as above with 100 nM ^{3}H-MT2 at 37°C for 1 hour, washed and lysed with NH_4Cl.

III.8. Myocardial ischemia model

Myocardial ischemia was induced in the mouse by ligating the left coronary artery, a method previously used in this species[73]. 6–8 week-old C57BL/6J male mice (Jackson

Laboratories, Bar Harbor, ME) were initially anesthetized with intraperitoneal injections of ketamine (100 mg/kg) and xilazine (5 mg/kg) and ventilated through a nose cone with a tidal volume of 0.2 ml at 120 breaths/min using a rodent respirator (Model 683; Harvard Apparatus, South Natick, MA). A median sternotomy will be performed, and the proximal left anterior descending coronary artery (LAD) will be visualized and ligated with 8-0 silk suture (BV-1, Ethicon). Ischemia was confirmed by the appearance of hypokinesis and pallor distal to the occlusion. 29 minutes later an intramuscular injection of MT2 (2mg/kg) was performed. After 30 minutes of LAD occlusion, the ligature was removed, and reperfusion was visually confirmed. The chest wall was closed, and the mice recovered in a temperature-controlled area for 24 hours.

III.9. Quantification of infarct size

After the 24h reperfusion the LAD was reoccluded and 1% Evans blue is perfused into the aorta and coronary arteries with distribution throughout the ventricular wall. The left ventricle of each heart is excised and weighed. It was sliced parallel to the atrioventricular groove into 2- to 3-mm-thick sections for demarcation of the viable and nonviable myocardium within the risk zone. The slices were incubated in p-nitroblue tetrazolium (NBT 0.5 mg/ml) solution prepared in pH 7.4 phosphate buffer for 40 min at 37°C. Subsequently, the slices were placed on a light table and photographed on both sides. Using the ImageJ software (NIH, Boston, MA, USA) the pictures were analysed and the different areas were delineated. Using the weights of the slices and the percentages of the different coloured areas, the percent of viable cardiac muscle (dark blue), area at risk AAR (red and white) and infarcted area (white) of the left ventricle (LV) were calculated. The infarct size was expressed as the ratio of infarct area and total area in the risk zone and the left ventricle.

III.10. Echocardiography assessment

In vivo transthoracic echocardiography of the left ventricle with use of a 15-MHz linear array transducer interfaced with a Sonos 5500 will be performed at different time points.

For each mouse, two measurements were performed: before (baseline) LAD occlusion and after 24 h of reperfusion. To assess ventricular function, two parameters were employed: ejection fraction (EF) (cardiac output/LV diastolic volume) was determined by the Vivid i LV function software; fractional shortening (FS) which takes into consideration one 2D cross section of the heart. Specifically, in the M-mode records, the LV intraventricular diameters (LVID) were measured at systole and diastole (LVIDs and LVIDd, respectively), and LV%FS was calculated as follows: LV%FS=[(LVIDs − LVIDd)/ LVIDd]×100.

IV. RESULTS

IV.1. NGF-mimetic activities of MT2 in TrkA$^+$ cells

IV.1.1. Screening of the chemical library

A chemical library of compounds was synthesized based on the spatial conformation of the binding site for NGF in TrkA[71]. Over 150 compounds were screened based on their ability to maintain the survival of PC12 cells cultured in serum-free conditions by using the MTT (thiazolyl blue tetrazolium bromide) assay and human recombinant NGF (hrNGF) as internal standard. Based on the survival promoting activity four compounds with high, dose-dependent, NGF-mimetic activity were selected (figure 3**a**) and screened for their capacity to maintain the survival of different cell types or to induce different NGF-induced functions as the induction of VGF gene[68]. The compound 11, named MT2 was the most active compound in all these assay. Thus we used MT2 in all the following experiments. The chemical structure of MT2 compound is reported in figure 3**b**.

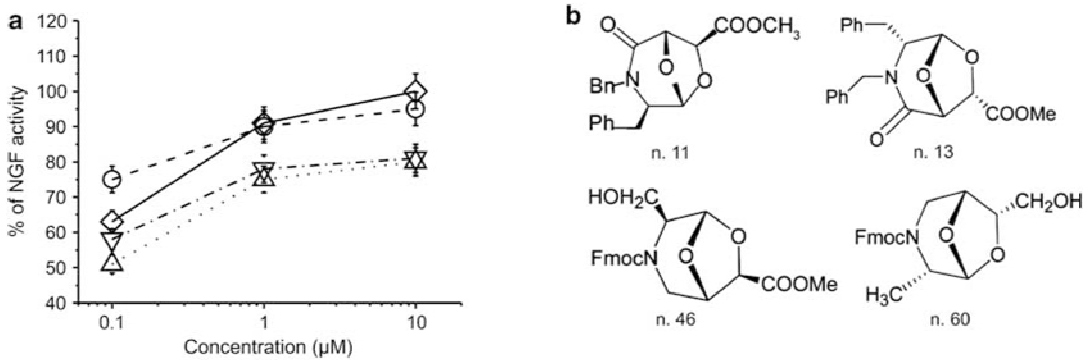

Figure 3: NGF mimetic activity of selected compounds[68]. (**a**) PC12 cells were cultured for 72 h in serum-free medium in the presence or absence of the indicated concentrations of compounds n. 11 (○), 13 (△), 46 (▽), 60 (◇), or 4 nM hrNGF as positive control. Cell survival was measured as MTT incorporation of triplicate cultures and expressed as percentage of the survival activity induced by hrNGF. Results of four different experiments (mean±S.E.) are reported. (**b**) Structural formula of the compounds n. 11, 13, 46, 60. Compound n. 11 was named MT2.

IV.1.2. Modulation of the apoptotic process

It is known that serum-deprivation of cells normally cultured in serum-supplemented media is a type of metabolic stress which easily induces the apoptotic death through the activation of the intrinsic pathway. Thus, in order to explain the survival-promoting activities of NGF-mimetic compounds we wanted to study the effects of MT2 in preventing the apoptotic death.

First we studied whether MT2 could prevent the surface exposure of phosphatidyl-serine, an early event of the apoptotic process, in PC12 cells cultured in absence of serum and compared the MT2 effects with those induced by hrNGF. The surface exposure of phosphatidyl-serine in PC12 cells was revealed by staining with FITC annexin V and measured by cytofluorimetry. The results shown in figure 4 indicated that MT2 is able to decrease the exposure of phosphatidyl-serine in PC12 cells in a dose dependent fashion and at levels even higher than those obtained by optimal concentrations of hrNGF.

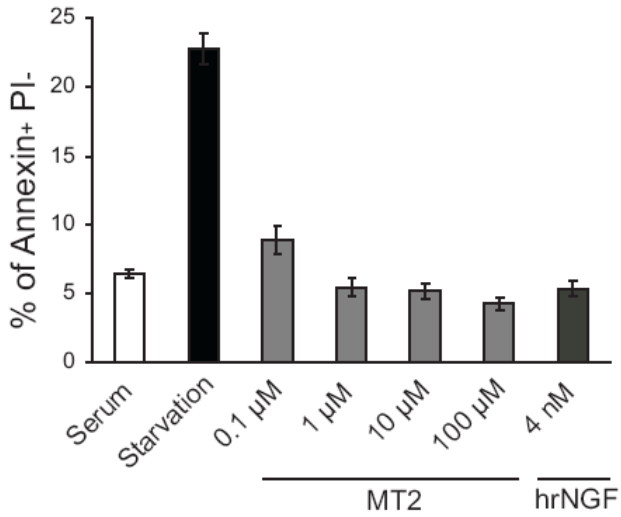

Figure 4: Effect of MT2 on apoptosis induced by serum starvation[68]. PC12 cells were cultured in serum-free medium in the presence or absence of different concentrations of MT2 or 4 nM hrNGF as positive control. Cells were washed, stained with FITC Annexin V/PI and the percentage of $Annexin^{+}PI^{-}$ cells recorded by cytofluorimetry. Statistical analysis, performed by Student's t-test shows significant differences (p at least < 0.01) between untreated versus treated (any concentration) starved cultures.

IV.1.3. Interaction with TrkA receptor

To assess whether MT2 could specifically interact with TrkA, we set up initial binding studies with ^{125}I-NGF on PC12 cells and tested MT2 for its ability to displace the binding of fixed amounts of iodinated NGF. Analysis of binding data showed that MT2 was able to displace the binding of ^{125}I-NGF in the nanomolar range of concentration (figure 5**a**). Nevertheless, these results did not conclusively demonstrate that MT2 really binds to TrkA.

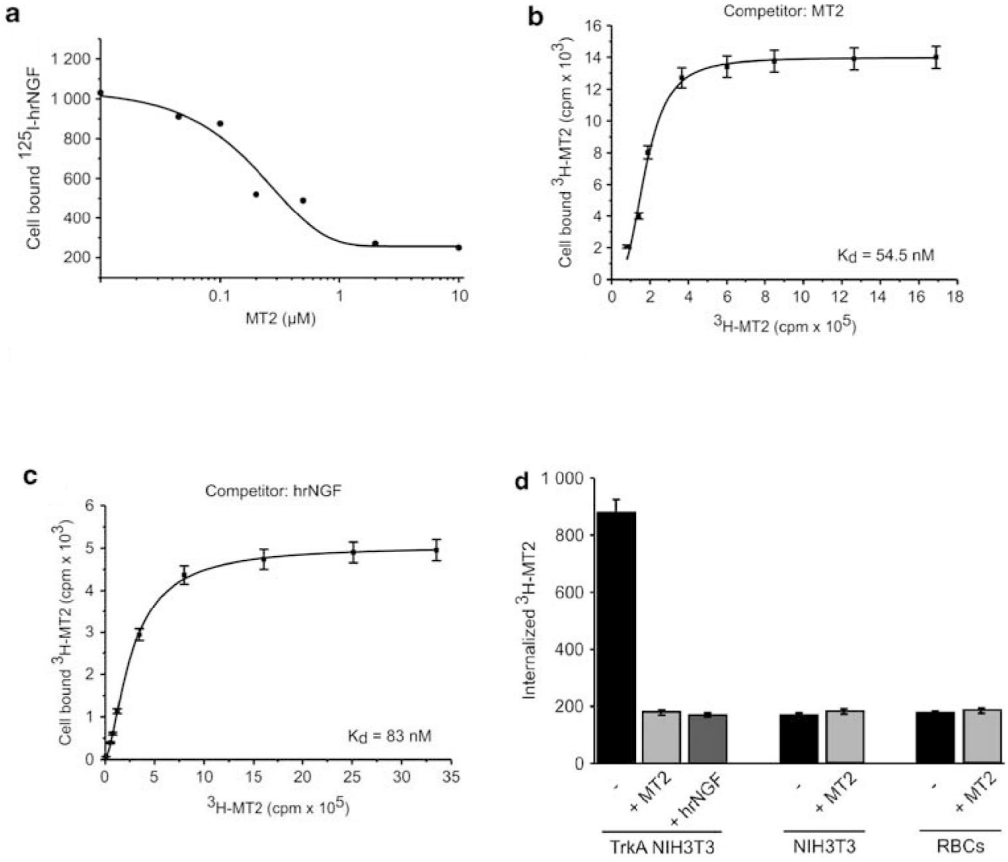

Figure 5: MT2 interactions with TrkA[68]. (a) Displacement of ^{125}I-hrNGF bound to PC12 cells by MT2. PC12 cells were incubated with 0.1 nM ^{125}I-hrNGF in the presence or absence of different concentrations of MT2. Specific cell bound radioactivity was calculated and the results analyzed by Origin software. Results of one representative experiment out of three performed are shown. (**b** and **c**) Binding of ^{3}H-MT2 to TrkA NIH-3T3. NIH-3T3, stably transfected with full-length human TrkA, were incubated in triplicate with different concentrations of ^{3}H-MT2, in the presence or absence of excess cold MT2 (**b**) or 4 nM cold hrNGF (**c**). Specific cell bound radioactivity was calculated and the results analyzed by the Origin software (one-site binding assay). (**d**) Internalization of 3H-MT2. TrkA-NIH-3T3 or mock-transfected cells were incubated for 1 h at 4 °C with ^{3}H-MT2 in the presence or absence of excess cold MT2 or hrNGF. Then, cells were washed and brought at 37 °C for 1 h. Membrane radioactivity was eluted with 0.1M glycine buffer, pH 2.8. RBC were incubated for 1 h at 37 °C with ^{3}H-MT2 in the presence or absence of excess cold MT2 or hrNGF. Cells were lysed, and cell-bound radioactivity recorded. Data are expressed as mean bound radioactivity ± S.E. of triplicate cultures. Results of one representative experiments out of three performed are shown.

To obtain evidences on the direct binding of MT2 to TrkA, we transfected plasmids coding human full length TrkA chain or empty vectors into NIH-3T3 cells and obtained stable transfectants. Then we labeled MT2 with tritium (^{3}H-MT2) and used it for binding experiments with TrkA NIH-3T3 and NIH-3T3cells. The data obtained showed that a saturation curve of ^{3}H-MT2 binding was evident only in TrkA transfected cells but not in cells transfected with the empty vector (data not shown) and the analysis of binding data revealed K*d* values ranging between 50 and 100nM (figure 5**b**, **c**). We also obtained data on MT2 internalization by culturing cells at 37°C with the ^{3}H-MT2 in the presence or absence of excess cold MT2 or hrNGF. These data showed that the internalization of ^{3}H-MT2 occurred in TrkA NIH-3T3 cells, but not in mock-transfected cells (transfected with empty vector) and, again, labeled MT2 internalization was blocked by hrNGF (figure 5**d**). Furthermore, by using human eritrocytes (RBC), we demonstrated the absence of aspecific ^{3}H-MT2 internalization (figure 5**d**).
So, this set of experiments demonstrated that MT2 molecule was able to bind TrkA and to undergo to subsequent receptor-mediated internalization in a specific manner since both phenomena were antagonized by the native neurotrophin. Furthermore MT2 failed to passively diffuse through cellular membranes.

IV.1.4. Biochemical pathways activated by MT2 in TrkA$^+$ cells

The first demonstrable event upon NGF binding to TrkA is autophosphorylation of the receptor. To ascertain whether such event is induced by MT2, we studied TrkA phosphorylation through the evaluation of specific tyrosine (490, 674/675 and 785) present in the intracellular domain of the receptor. The western blot analysis showed that the binding of MT2 to TrkA receptor induces a significant phosphorylation of tyrosine 490 and only a minimal activation of tyrosine 674/675 and 785, suggesting that biological responses induced by MT2 could not completely overlap with those induced by NGF (figure 6**a**).

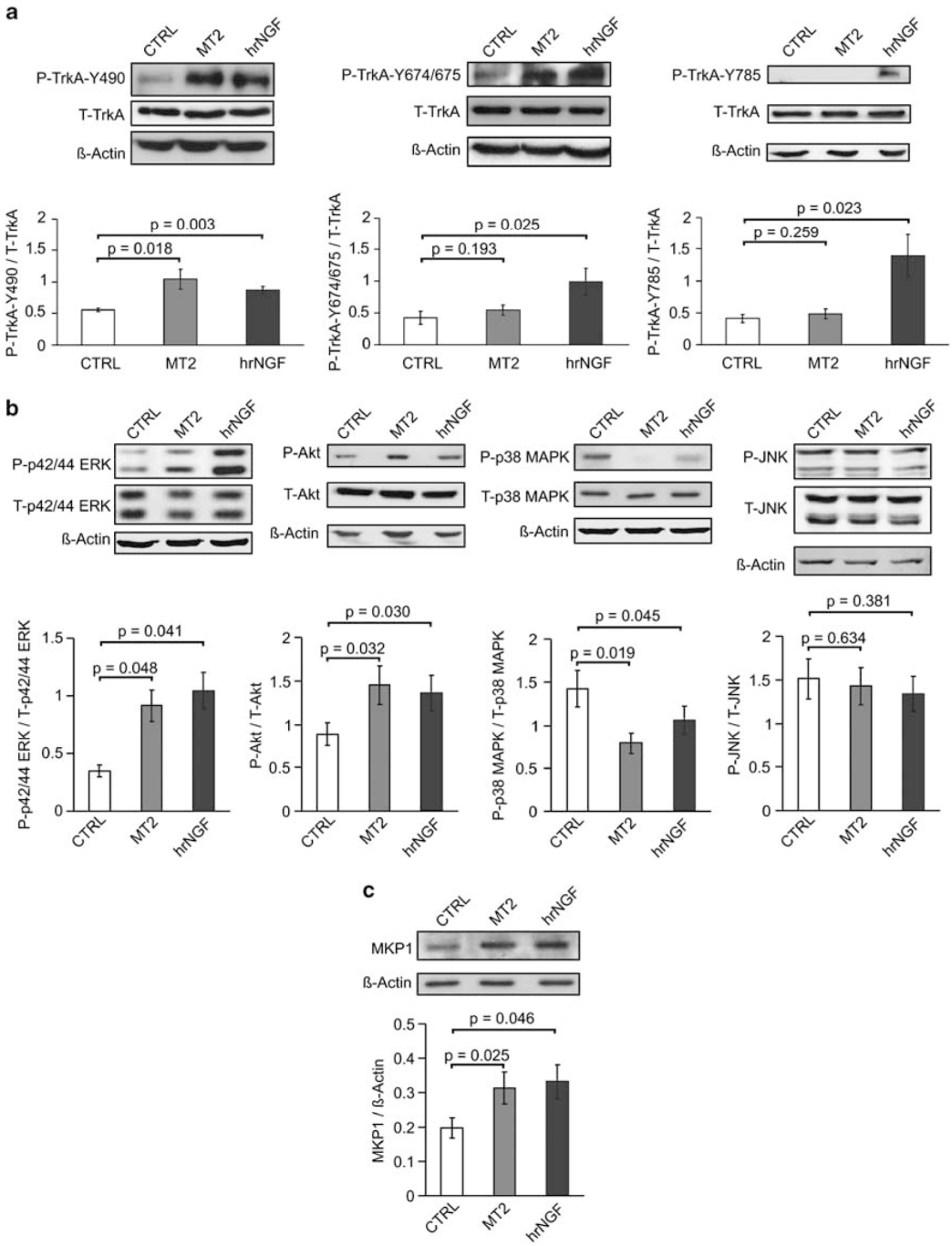

Figure 6: Biochemical pathways induced by MT2 in PC12 cells[68]. (**a**) TrkA phosphorylation. Serum-starved PC12 cells were stimulated with 10 µM MT2, or 4 nM hrNGF as positive control, for 15 min. Cells lysates were blotted with antibodies to P-Y490, P-Y674/675, P-Y785 and with anti-actin as loading control. Membranes were stripped and stained with anti-total TrkA IgG. The relative histograms represent the data of densitometric analysis and are expressed as the ratio between phosphoprotein (P) and total protein (T) of five different experiments (mean±S.E.). Statistical analysis was performed by paired Student's t-test. (**b**) Kinases phosphorylation. Serum-starved PC12 cells were stimulated with 10 µM MT2, or 4 nM hrNGF, for 30 min. Cell lysates were blotted with rabbit anti-P-ERK1/2, anti-P-Akt, anti-P-p38 MAPK, anti-P-JNK. Then, membranes were stripped and stained with antibodies to the respective total protein and with anti-actin antibodies as loading control. The relative histograms represent the data of densitometric analysis and are expressed as the ratio between phosphoprotein (P) and total protein (T) of five different experiments (mean±S.E.). Statistical analysis was performed by paired Student's t-test. (**c**) Phosphatase. Serum-starved PC12 cells were stimulated with 10 µM MT2, or 4 nM hrNGF as positive control, for 30 min. Cell lysates were blotted with rabbit anti-MKP1 IgG and anti-actin antibodies as loading control. The relative histogram represents the data of densitometric analysis and is expressed as the ratio between MKP1 expression and actin of five different experiments (mean±S.E.). Statistical analysis was performed by paired Student's t-test.

Upon phosphorylation of Tyr490 of TrkA receptor by NGF, the MAP kinase cascade, a pathway central in regulating death/survival, is activated. Therefore we studied the phosphorylation status of different kinases with opposite functions belonging to MAPK pathway such as ERK, c-Jun N-terminal kinases (JNK), p38 MAPK proteins, and of Akt, another kinase involved in the regulation of cell survival, in serum-starved PC12 cells exposed to MT2 or to hrNGF as control. As shown in figure 6**b** the data obtained in these experiments revealed that ERK1/2 and Akt became strongly activated upon addition of either NGF and MT2. Conversely, MT2 – or hrNGF as control – induced a marked dephosphorylation of p38 MAPK. JNK activation was also reduced by MT2, but not at significance levels.

To investigate the mechanisms on the basis of the strong modulation of p38 MAPK activation induced by MT2, we studied the expression of MKP-1, a phosphatase which dephosphorylates p38 MAPK and also JNK (with lesser affinity). We observed that the exposure of starved PC12 cells to MT2 or NGF caused a marked increase in MKP-1 protein levels, as early as 30 min after stimulation (figure 6**c**).

Thus following the binding of MT2 with TrkA, a metabolic pathway including MKP-1 function, p38 MAPK and JNK dephosphorylation is activated and this pathway is likely related to apoptosis inhibition as shown in different cellular type.

IV.2. NGF-mimetic activities of MT2 in cardiomyocytes

IV.2.1. Modulation of the apoptotic process in cardiomyocytes

Several studies have reported the protective role of NGF in experimental models of acute I/R[58;70]. The NGF-mediated protection is mainly based on the anti-apoptotic effects of the neurotrophins exerted on cardiomyocytes and on endothelial cells[58] during the reperfusion phase when large amounts of oxygen radicals activate the intrinsic pathway of apoptosis.

Thus we wanted to investigate whether MT2 could also protect cardiomyocytes in I/R condition. In this regard, we used H9C2 cell line that were differentiated in cardiomyocytes using retinoic acid and incubated them in oxygen glucose deprivation

(OGD) for 1 hour to mime ischemic conditions. Cells were then incubated in normoxia with fresh medium in presence or absence of 10 μM MT2.

We first quantified PARP cleavage and caspase 3 activation as markers of the apoptotic damage through western blot analysis after 24-hour reperfusion period. Figure 7 shows that MT2 inhibited PARP cleavage and caspase 3 activation thus maintaining cardiomyocytes cell survival.

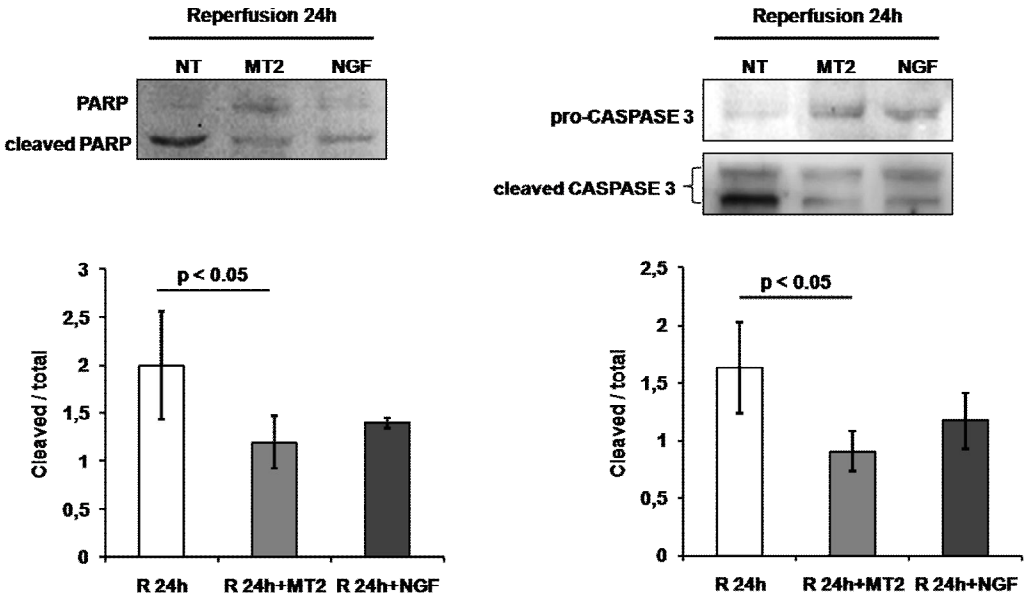

Figure 7: Effect of MT2 on apoptosis induced by ischemia/reperfusion in cardiomyocytes. H9C2 cells were differentiated in cardiomyocytes with 1% horse serum + 10 nM of retinoic acid added daily for 6 days and incubated in deep hypoxia (~0.1% O_2) for 1 hour in PBS with Ca^{2+}/Mg^{2+}. Cells were then incubated in normoxia with fresh medium with or without 10 μM MT2 for 24 hours (24h). Total cell lysates in RIPA buffer were subjected to immuno-blotting with an antibodies anti-PARP or anti-CASPASE 3. The relative histograms represent the data of densitometric analysis and are expressed as the ratio between cleaved and total-protein of three different experiments (mean±S.E.). Statistical analysis was performed by paired Student's t-test.

It's known that many highly conserved serine/threonine mitogen-activated protein kinases (MAPK), including p38 MAPK, are activated in response to myocardial I/R. p38 MAPK activation has been shown to accentuate myocardial injury and impair cardiac function. Thus we studied whether MT2 treatment could interfere with MAPK activation, in particular with ERK1/2 and p38 activation in cardiomyocytes undergoing reperfusion following OGD.

Figure 8 shows the results of western blot analysis with specific antibodies to phospho-ERK1/2 and phospho-p38 MAPK performed in lysates of cardiomyocytes subjected to OGD and cultured in normoxic condition for 24 hours. The data show an increase in

ERK1/2 phosphorylation and a marked dephophorylation of p38 MAPK in MT2 treated cells compared to untreated cells.

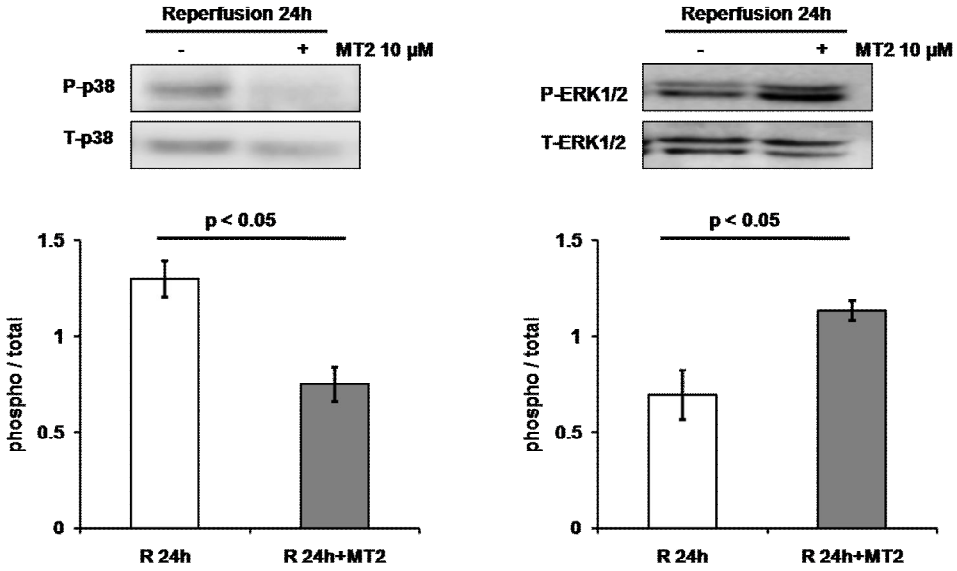

Figure 8: Effect of MT2 on p38 MAPK and ERK1/2 phosphorylation in cardiomyocytes. H9C2 cells were differentiated in cardiomyocytes with 1% horse serum + 10 nM of retinoic acid added daily for 6 days and incubated in deep hypoxia (~0.1% O_2) for 1 hour in PBS with Ca^{2+}/Mg^{2+}. Cells were then incubated in normoxia with fresh medium with (+) or without (-) 10 µM MT2 for 24 hours (Reperfusion 24h). Cell lysates were blotted with rabbit anti-P-p38 and anti-P-ERK1/2. Then, membranes were stripped and stained with antibodies to the respective total protein. The relative histograms represent the data of densitometric analysis and are expressed as the ratio between phosphoprotein (P) and total protein (T) of three different experiments (mean±S.E.). Statistical analysis was performed by paired Student's t-test.

To investigate whether MKP-1 is involved in MT2-induced deactivation of p38 MAPK in cardiomyocytes subjected I/R we treated cardiomyocytes as above (OGD and normoxia for 1 or 24 hours) and studied the expression of MKP-1 in cell lysates through western blot analysis with specific antibodies. Figure 9 shows that MT2 was able to increase the expression of MKP-1. Taken together these data suggest that MT2 has marked trophic effects on cardiomyocytes under I/R condition.

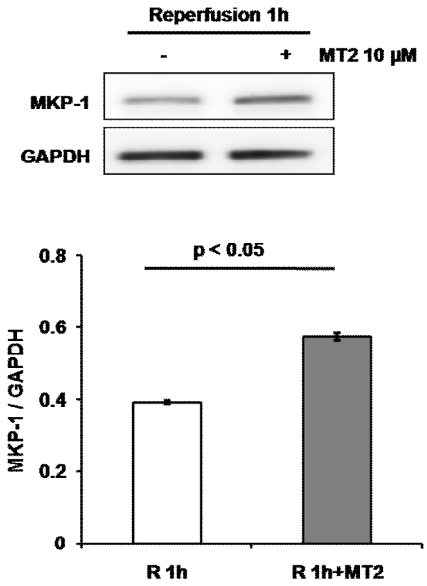

Figure 9: Effect of MT2 on MKP-1 expression in cardiomyocytes. H9C2 cells were differentiated in cardiomyocytes with 1% horse serum +10 nM of retinoic acid added daily for 6 days and incubated in deep hypoxia (~0.1% O_2) for 1 hour in PBS (with Ca^{2+}/Mg^{2+}). Cells were then incubated in normoxia with fresh medium with (+) or without (-) 10 µM MT2 for 1 hour (Reperfusion 1h). Cell lysates were blotted with rabbit anti-MKP-1 and anti-GAPDH antibodies as loading control. The relative histogram represents the data of densitometric analysis and is expressed as the ratio between MKP-1 and GAPDH protein of three different experiments (mean±S.E.). Statistical analysis was performed by paired Student's t-test.

IV.2.2. Effect of MT2 on HIF-1α/VEGF pathway

Different survival mechanisms could be activated during ischemia conditions; among these VEGF plays an important role on the overall cell survival[57]. The VEGF production is largely dependent on HIF-1α, (Hypoxia-Inducible Factor). Thus we wanted to investigate the role of MT2 in HIF-1α/VEGF pathway. H9C2 differentiated in cardiomyocytes were incubated in hypoxia for 1 hour, cells were then incubated in normoxia in presence or absence of 10µM MT2 for 1 h or 24 hours. The data obtained demonstrated that during the reperfusion phase MT2 increased HIF-1α expression before the first hour (figure 10). Consequently, after 24 hours of reperfusion MT2 treatment was able to increase VEGF-A protein levels (figure 10).

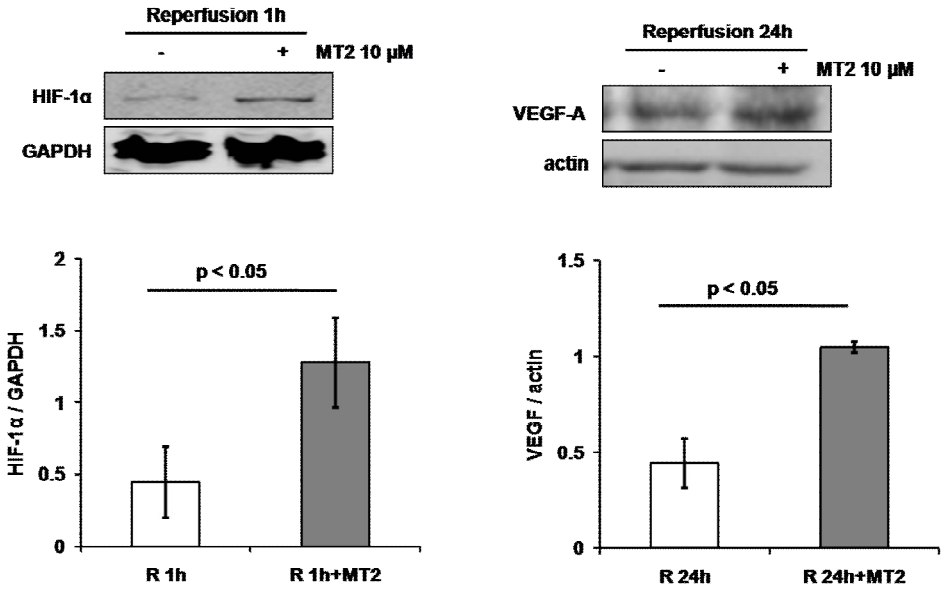

Figure 10: Effect of MT2 on HIF-1α / VEGF pathway in cardiomyocytes. H9C2 cells were differentiated in cardiomyocytes with 1% horse serum + 10 nM of retinoic acid added daily for 6 days and incubated in hypoxia (~0.1% O_2) for 1 hours in PBS with Ca^{2+}/Mg^{2+} (OGD 1h). Then cells were incubated in normoxia with fresh medium with (+) or without (-) 10 µM MT2 for 1 or 24 hours. Cell lysates were blotted with anti HIF-1α or anti-VEGF and anti-GAPDH or anti-actin antibodies as loading control. The relative histograms represent the data of densitometric analysis and are expressed as the ratio between HIF-1α and GAPDH protein or VEGF and actin protein of three different experiments (mean±S.E.). Statistical analysis was performed by paired Student's t-test.

IV.2.3. Inhibition of HIF-1α

To confirm the activation of HIF-1α/VEGF pathway, we used Acriflavine (ACF), a pharmacological inhibitor of HIF-1α/HIF-1β dimerization.

H9C2 differentiated in cardiac cells were incubated in OGD for 1 hour in presence or absence of 5 µM ACF and then incubated in normoxia with fresh medium for 1 hour or 24 hours. During the reperfusion phase cells were treated with or without 10 µM MT2. Western blot analysis showed that ACF was able to block HIF-1α expression also in the presence of MT2 and consequently VEGF-A production (figure 11).

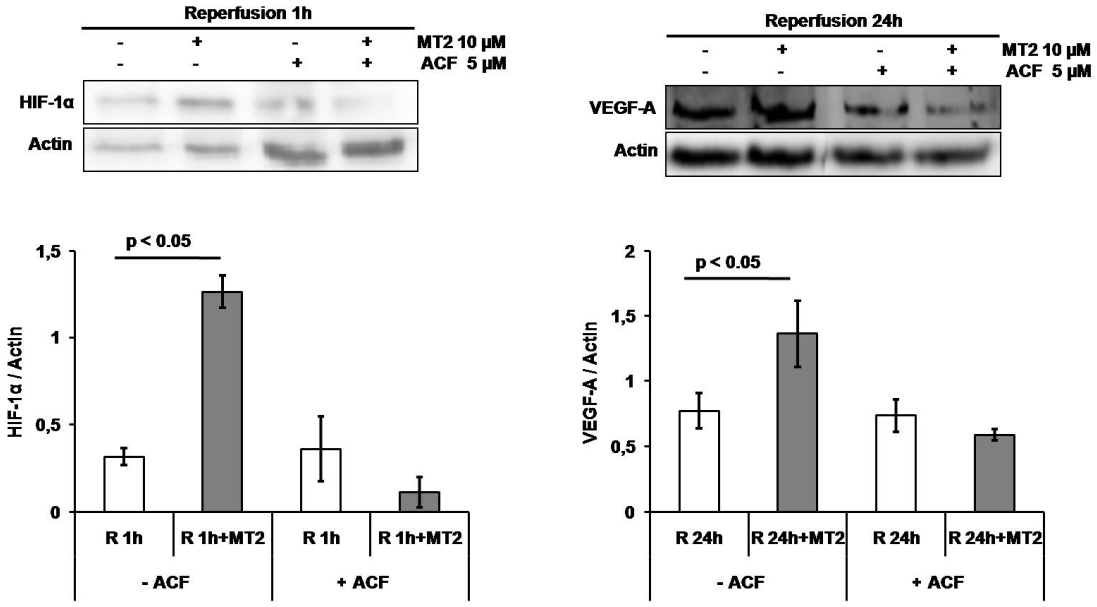

Figure 11: Effect of Acriflavine on HIF-1α expression induced by MT2 in cardiomyocytes. H9C2 cells were differentiated in cardiomyocytes with 1% Horse Serum (HS) + 10 nM of Retinoic Acid added daily for 6 days and incubated in hypoxia (~0.1% O_2) for 1 hours in PBS with Ca^{2+}/Mg^{2+} (OGD 1h). Then cells were incubated in normoxia with fresh medium with (+) or without (-) 10 µM MT2 for 1 or 24 hours. Acriflavine (ACF, 5 µM) was added for 1 hour during the ischemic phase to inhibit HIF-1α. Cell lysates were blotted with antibodies anti HIF-1α or anti-VEGF and anti-actin antibody as loading control. The relative histograms represent the data of densitometric analysis and are expressed as the ratio between HIF-1α or VEGF and actin protein of three different experiments (mean±S.E.). Statistical analysis was performed by paired Student's t-test.

IV.2.4. In vivo *Study Design*

Based on the data obtained in *in vitro* models of I/R of cardiomyocytes, we wanted to investigate whether MT2 could exert protective activity in *in vivo* models of myocardial ischemia in mice.

Myocardial ischemia was induced by the ligation of the left anterior descending (LAD) branch of the coronary artery in groups of 10 C57BL/6J mice. The experimental protocol used included a preliminary echocardiographic assessment of each animal, followed by a 30-minute LAD artery ligation, intramuscular injection of MT2 (2mg/kg) 1 minute before removal of ligation, and a 24-hour reperfusion period. Control groups of mice were treated with PBS alone (vehicle).

The myocardial function of each animal was then re-assessed by echocardiography and mice were sacrificed to obtain histopathologic samples (figure 12).

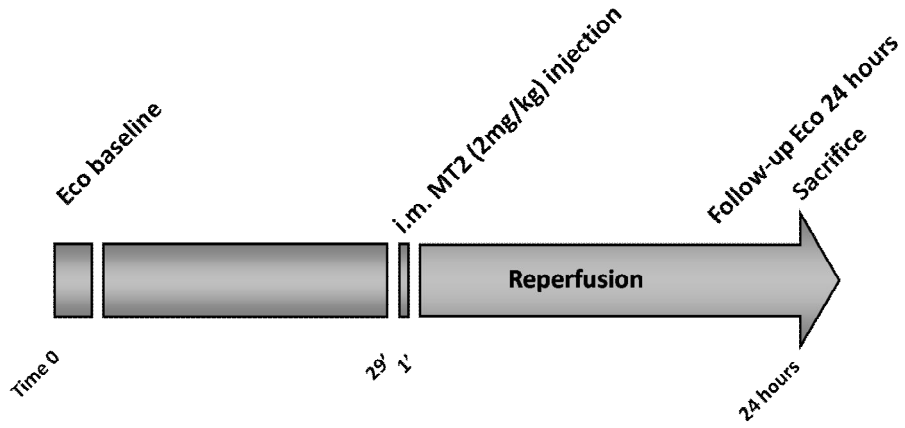

Figure 12: Study design of myocardial infarction.

IV.2.5. MT2 treatment decreases the size of infarct area in experimental model of myocardial ischemia in mice

Before heart removal, heart was stained *in vivo* with Even Blue dye to discriminate the viable area from area at risk. Then heart was rapidly excised from the thorax and the left ventricle was isolated and cut into slices perpendicular to the axis of the LAD coronary artery. To distinguish between the area at risk and infarcted area, slices were incubated in p-nitroblue tetrazolium that in the presence of intact dehydrogenase enzyme systems forms red-colored precipitates, while death tissue lacking of dehydrogenase activity appears white. The results showed that animals treated with MT2 revealed a marked reduction of the infarct area (of about 50%) compared to vehicle-treated animals (figure 13).

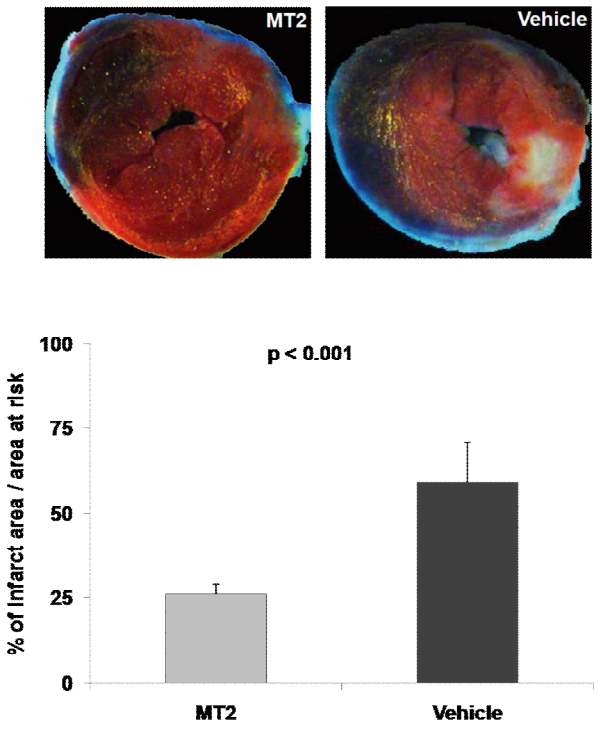

Figure 13: MT2 reduced the infarct size in ischemia and reperfusion (I/R) mouse. Representative pictures of ventricular slices from mice treated with PBS (vehicle) or MT2 (2mg/kg) as described in Methods. The area at risk (AAR) and infarct regions were determined at 24 h after reperfusion. Blu stain = viable area; red stain = area at risk (AAR) and white area = infarcted area. The infarct size normalized to the AAR (%). Each bar represents the mean±S.E of the I/R of 10 mice for different groups.

IV.2.6. MT2 improves myocardial functional parameters after I/R injury

Before sacrifice, the functional parameters investigated showed clear improvements: the Fractional Shortening in animals treated with MT2 remained of about 35% while in PBS-treated animals it was reduced closed 20% (figure 14**a**). Consistently, the Ejection Fraction was almost normalized upon treatment with MT2, compared to PBS-treated controls (figure 14**b**). We also obtained similar results in additional set of experiments with seven days follow up (data not shown).

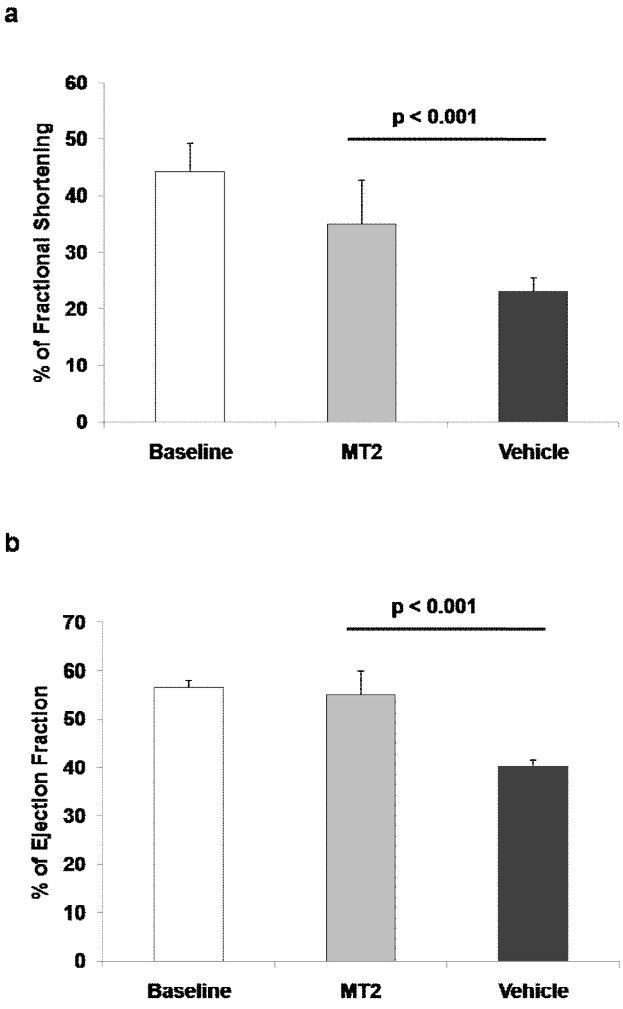

Figure 14: MT2 attenuated the decline in ventricular function in ischemia and reperfusion. (a) and **(b)** represent Fractional shortening and Ejection fraction obtained at baseline and 24 h post-I/R, in mice treated with 2mg/kg of MT2 or PBS (vehicle). I/R + MT2 (n = 10), I/R + PBS (n = 10).

V. DISCUSSION

Acute myocardial infarction (AMI) remains a leading cause of morbidity and mortality worldwide. For patients presenting with an AMI, early and successful myocardial reperfusion through thrombolytic therapy or primary PCI is the most effective interventional strategy for reducing infarct size and improving clinical outcomes. Surprisingly, the process of reperfusion might in itself induces myocardial injury, thereby reducing the beneficial effects of myocardial reperfusion. Cardiomyocytes' death is associated with the irreversible form of myocardial reperfusion injury leading to heart failure. For this reason, myocardial reperfusion injury would be expected to adversely affect clinical outcomes after an AMI, and it may contribute to mortality despite early and successful reperfusion. Although new antiplatelet and antithrombotic agents might improve myocardial reperfusion, there is still no effective therapeutic strategy for preventing myocardial reperfusion injury.

NGF was reported to be active in maintenance cardiomyocytes survival in I/R injury; however the use of recombinant cytokine as therapeutic tool was not encouraged due to the poor pharmacokinetic profile and to high cost. In this thesis we characterized the biochemical pathways activated by a NGF-mimetic compound, called MT2, strongly active in typical NGF-dependent assays, and tested its efficacy in preventing cardiomyocytes'death and in preserving cardiac function in experimental models of acute myocardial I/R.

We observed that MT2 is able to bind TrkA receptor at nanomolar concentrations and to induce conformational modifications of the receptor molecule sufficient to trigger its autophosphorylation, predominantly at tyrosine 490 and, to a lower extent, at tyrosine 785 and tyrosine 674/675. These data suggest that biological responses induced by MT2 could not completely overlap with those induced by NGF. Indeed we found that a reduced differentiative response of neural cells originate from MT2 signaling while the trophic activity of NGF are induced by MT2 even with more efficacy than NGF[68].

Binding and internalization experiments of labeled MT2 clearly show that the compound is specifically internalized by cells expressing TrkA receptor, while it does not permeate in aspecific manner cell membranes, being therefore unable to reach the cellular cytosolic compartment. These properties underscore the possibility to use MT2 as NGF-mimetic compound in therapeutic strategies.

We also characterized the biochemical pathways activated by MT2 following interaction with TrkA in NGF-responsive cells (PC12, TrkA NIH3T3). An early event induced by MT2 is the brisk and intense increase in the expression of MKP-1, a phosphatase specifically devoted to the modulation of the activity of p38 MAPK and JNK, two kinases critically involved in the activation of apoptotic process through the intrinsic pathway. A further important event induced by MT2 is a definite increase in the phosphorylation levels of kinases of the ERK family (in particular ERK1/2), enzymes critically involved in maintaining cell survival.

Activation of p38 MAPK and JNK and induction of apoptosis is described also in cardiomyocytes subjected to metabolic stress[54;74]. Thus, considering the antiapoptotic role of NGF in heart injury we wanted to test whether MT2 could protect cardiomyocytes in acute ischemia/reperfusion conditions.

For these experiments we selected the largely used H9C2 cell line[75] as representative of cardiomyocytes and OGD as method to mime acute ischemia event[76].

By using this experimental model we observed that MT2, administered during reperfusion phase, is able to modulate p38 MAPK activation and to decrease PARP cleavage and caspase 3 activation, thus maintaining the survival of cardiomyocytes. These results strongly indicate that MT2 could inhibit the apoptotic process induced by intracellular ROS accumulation during the reperfusion phase. Moreover the administration of MT2 at the beginning of the reperfusion phase (normoxia) induces a marked elevation and stabilization of HIF-1α (the regulatory subunit of the important transcription factor), likely attributable to its phosphorylation by ERK1/2.

As known HIF-1α is a transcription factor involved in VEGF gene expression[77]. Indeed the increase of HIF-1α induced by MT2 also caused a marked *de novo* synthesis and secretion of VEGF.

VEGF, a 45 kDa polypeptide, is a major regulator of angiogenesis in the heart but it also exerts a diverse variety of pleiotropic effects which include an acute cardioprotective effect[57]. Indeed VEGF, generated in response to myocardial ischemia,

binds to two high-affinity tyrosine kinase receptors, the flt-1 and the KDR (the human homologue of the murine flk-1 receptor), which are preferentially distributed on vascular endothelial cells but are also known to be present on cardiomyocytes[78;79].

The efficacy of MT2 in ischemia reperfusion injury was confirmed in *in vivo* experiments using a classical model of acute myocardial ischemia in mice, induced by the ligation of the left anterior descending (LAD) branch of the coronary artery[80]. Animals treated with intramuscular injection of MT2 at the beginning of reperfusion phase showed a marked reduction (> 50%) of the infarct area compared to animals treated with vehicle. Furthermore the values of fractional shortening in animals treated with MT2 ranged about 35 % of normal values while in animals treated with vehicles it dropped to ~20%. To note that 35% of fractional shortening is considered a limit allowing performance levels sufficient for autonomous life in humans. Consistently ejection fraction was almost normalized in animals treated with MT2 but not in controls. Thus both contractile parameters were positively affected by the pharmacologic treatment, at very high significance levels.

Although these data support the use of MT2 as therapeutic tool in acute myocardial ischemia, we think that further data, using mini-pigs as experimental models, need to be collected. Indeed, in this model infarct is induced by catether ballon inflation and drug is administered using the same device at the reperfusion. Furthermore the size of animals will allow a more precise quantification of myocardial apoptosis through NMR imaging and, therefore, a more reliable assessment of the achievements afforded by MT2 therapy.

VI. BIBLIOGRAPHY

1. Chen J, Hsieh AFC, Dharmarajan K, et al. National Trends in Heart Failure Hospitalization After Acute Myocardial Infarction for Medicare Beneficiaries 1998-2010. Circulation 2013;128:2577-84.
2. Yellon DM, Hausenloy DJ. Myocardial reperfusion injury - Reply. New England Journal of Medicine 2007;357:2409-10.
3. Hausenloy DJ, Yellon DM. Myocardial ischemia-reperfusion injury: a neglected therapeutic target. Journal of Clinical Investigation 2013;123:92-100.
4. Jennings RB, Sommers HM, Smyth GA, et al. Myocardial necrosis induced by temporary occlusion of a coronary artery in the dog. Arch Pathol 1960;70:68-78.
5. Dhalla NS, Elmoselhi AB, Hata T, Makino N. Status of myocardial antioxidants in ischemia-reperfusion injury. Cardiovascular Research 2000;47:446-56.
6. Doevendans PA, Daemen MJ, de Muinck ED, Smits JF. Cardiovascular phenotyping in mice. Cardiovascular Research 1998;39:34-49.
7. Theroux P, Chaitman BR, Danchin N, et al. Inhibition of the sodium-hydrogen exchanger with cariporide to prevent myocardial infarction in high-risk ischemic situations - Main results of the GUARDIAN trial. Circulation 2000;102:3032-+.
8. Erhardt LRW. GUARD during ischemia against necrosis (GUARDIAN) trial in acute coronary syndromes. American Journal of Cardiology 1999;83:23G-5G.
9. Avkiran M, Marber MS. Na+/H+ exchange inhibitors for cardioprotective therapy: Progress, problems and prospects. Journal of the American College of Cardiology 2002;39:747-53.
10. Jennings RB, Reimer KA. The Cell Biology of Acute Myocardial-Ischemia. Annual Review of Medicine 1991;42:225-46.

11. Hearse DJ, Bolli R. Reperfusion Induced Injury - Manifestations, Mechanisms, and Clinical Relevance (Reprinted from Trends in Cardiovascular Medicine, Vol 1, Pg 233-40, 1991). Cardiovascular Research 1992;26:101-8.
12. Dhalla NS, Saini HK, Tappia PS, et al. Potential role and mechanisms of subcellular remodeling in cardiac dysfunction due to ischemic heart disease. Journal of Cardiovascular Medicine 2007;8:238-50.
13. Hoffman JW, Jr., Gilbert TB, Poston RS, Silldorff EP. Myocardial reperfusion injury: etiology, mechanisms, and therapies. J Extra Corpor Technol 2004;36:391-411.
14. Kloner RA, Bolli R, Marban E, et al. Medical and cellular implications of stunning, hibernation, and preconditioning - An NHLBI Workshop. Circulation 1998;97:1848-67.
15. Krug A, Du Mesnil dR, Korb G. Blood supply of the myocardium after temporary coronary occlusion. Circ Res 1966;19:57-62.
16. Ito H. No-reflow phenomenon and prognosis in patients with acute myocardial infarction. Nature Clinical Practice Cardiovascular Medicine 2006;3:499-506.
17. Kleinbongard P, Bose D, Baars T, et al. Vasoconstrictor Potential of Coronary Aspirate From Patients Undergoing Stenting of Saphenous Vein Aortocoronary Bypass Grafts and Its Pharmacological Attenuation. Circulation Research 2011;108:344-U172.
18. Manning AS, Hearse DJ. Reperfusion-induced arrhythmias: mechanisms and prevention. J Mol Cell Cardiol 1984;16:497-518.
19. Piper HM, Garcia-Dorado D, Ovize M. A fresh look at reperfusion injury. Cardiovascular Research 1998;38:291-300.
20. Bersohn MM, Morey AK, Weiss RS. Sarcolemmal calcium transporters in myocardial ischemia. Journal of Molecular and Cellular Cardiology 1997;29:2525-32.
21. Schafer C, Ladilov Y, Inserte J, et al. Role of the reverse mode of the Na+/Ca2+ exchanger in reoxygenation-induced cardiomyocyte injury. Cardiovascular Research 2001;51:241-50.
22. Klein HH, Pich S, Lindert S, et al. Treatment of Reperfusion Injury with Intracoronary Calcium-Channel Antagonists and Reduced Coronary Free

Calcium-Concentration in Regionally Ischemic, Reperfused Porcine Hearts. Journal of the American College of Cardiology 1989;13:1395-401.

23. Gumina RJ, Buerger E, Eickmeier C, et al. Inhibition of the Na+/H+ exchanger confers greater cardioprotection against 90 minutes of myocardial ischemia than ischemic preconditioning in dogs. Circulation 1999;100:2519-26.
24. Boden WE, van Gilst WH, Scheldewaert RG, et al. Diltiazem in acute myocardial infarction treated with thrombolytic agents: a randomised placebo-controlled trial. Lancet 2000;355:1751-6.
25. Zeymer U, Suryapranata H, Monassier JP, et al. The Na+/H+ exchange inhibitor eniporide as an adjunct to early reperfusion therapy for acute myocardial infarction - Results of the evaluation of the safety and cardioprotective effects of eniporide in acute myocardial infarction (ESCAMI) trial. Journal of the American College of Cardiology 2001;38:1644-50.
26. Hearse DJ, Humphrey SM, Chain EB. Abrupt reoxygenation of the anoxic potassium-arrested perfused rat heart: a study of myocardial enzyme release. J Mol Cell Cardiol 1973;5:395-407.
27. Zweier JL, Flaherty JT, Weisfeldt ML. Direct measurement of free radical generation following reperfusion of ischemic myocardium. Proc Natl Acad Sci U S A 1987;84:1404-7.
28. Murphy E, Steenbergen C. Preconditioning: The mitochondrial connection. Annual Review of Physiology 2007;69:51-67.
29. Hess ML, Okabe E, Kontos HA. Proton and free oxygen radical interaction with the calcium transport system of cardiac sarcoplasmic reticulum. J Mol Cell Cardiol 1981;13:767-72.
30. Zweier JL, Talukder MA. The role of oxidants and free radicals in reperfusion injury. Cardiovasc Res 2006;70:181-90.
31. Effect of 48-h intravenous trimetazidine on short- and long-term outcomes of patients with acute myocardial infarction, with and without thrombolytic therapy; A double-blind, placebo-controlled, randomized trial. The EMIP-FR Group. European Myocardial Infarction Project--Free Radicals. Eur Heart J 2000;21:1537-46.
32. Crompton M. The mitochondrial permeability transition pore and its role in cell death. Biochemical Journal 1999;341:233-49.

33. Halestrap AP. The mitochondrial permeability transition: its molecular mechanism and role in reperfusion injury. Mitochondria and Cell Death 1999;66:181-203.
34. Halestrap AP, Mcstay GP, Clarke SJ. The permeability transition pore complex: another view. Biochimie 2002;84:153-66.
35. Halestrap AP, Clarke SJ, Javadov SA. Mitochondrial permeability transition pore opening during myocardial reperfusion - a target for cardioprotection. Cardiovascular Research 2004;61:372-85.
36. Griffiths EJ, Halestrap AP. Mitochondrial Nonspecific Pores Remain Closed During Cardiac Ischemia, But Open Upon Reperfusion. Biochemical Journal 1995;307:93-8.
37. Hausenloy DJ, Maddock HL, Baxter GF, Yellon DM. Inhibiting mitochondrial permeability transition pore opening: a new paradigm for myocardial preconditioning? Cardiovascular Research 2002;55:534-43.
38. Hausenloy DJ, Duchen MR, Yellon DM. Inhibiting mitochondrial permeability transition pore opening at reperfusion protects against ischaemia-reperfusion injury. Cardiovascular Research 2003;60:617-25.
39. Argaud L, Gateau-Roesch O, Muntean D, et al. Specific inhibition of the mitochondrial permeability transition prevents lethal reperfusion injury. J Mol Cell Cardiol 2005;38:367-74.
40. Skyschally A, Schulz R, Heusch G. Cyclosporine A at Reperfusion Reduces Infarct Size in Pigs. Cardiovascular Drugs and Therapy 2010;24:85-7.
41. Shanmuganathan S, Hausenloy DJ, Duchen MR, Yellon DM. Mitochondrial permeability transition pore as a target for cardioprotection in the human heart. American Journal of Physiology-Heart and Circulatory Physiology 2005;289:H237-H242.
42. Hausenloy DJ, Yellon DM. New directions for protecting the heart against ischaemia-reperfusion injury: targeting the Reperfusion Injury Salvage Kinase (RISK)-pathway. Cardiovascular Research 2004;61:448-60.
43. Hausenloy DJ, Yellon DM. Reperfusion injury salvage kinase signalling: taking a RISK for cardioprotection. Heart Failure Reviews 2007;12:217-34.

44. Yellon DM, Baxter GF. Reperfusion injury revisited - Is there a role for growth factor signaling in limiting lethal reperfusion injury? Trends in Cardiovascular Medicine 1999;9:245-9.
45. Matsui T, Li L, Wu JC, et al. Phenotypic spectrum caused by transgenic overexpression of activated Akt in the heart. Journal of Biological Chemistry 2002;277:22896-901.
46. Yue TL, Wang CL, Gu JL, et al. Inhibition of extracellular signal-regulated kinase enhances ischemia/reoxygenation-induced apoptosis in cultured cardiac myocytes and exaggerates reperfusion injury in isolated perfused heart. Circulation Research 2000;86:692-9.
47. Davidson SM, Hausenloy D, Duchen MR, Yellon DM. Signalling via the reperfusion injury signalling kinase (RISK) pathway links closure of the mitochondrial permeability transition pore to cardioprotection. International Journal of Biochemistry & Cell Biology 2006;38:414-9.
48. Abdallah Y, Gkatzoflia A, Gligorievski D, et al. Insulin protects cardiomyocytes against reoxygenation-induced hypercontracture by a survival pathway targeting SR Ca2+ storage. Cardiovascular Research 2006;70:346-53.
49. Hausenloy DJ, Tsang A, Yellon DM. The reperfusion injury salvage kinase pathway: A common target for both ischemic preconditioning and postconditioning. Trends in Cardiovascular Medicine 2005;15:69-75.
50. See F, Kompa A, Krum H. p38 MAP kinase as a therapeutic target in cardiovascular disease. Drug Discovery Today: Therapeutic Strategies 2004;1:149-54.
51. Clark JE, Sarafraz N, Marber MS. Potential of p38-MAPK inhibitors in the treatment of ischaemic heart disease. Pharmacology & Therapeutics 2007;116:192-206.
52. Young PR, McLaughlin MM, Kumar S, et al. Pyridinyl imidazole inhibitors of p38 mitogen-activated protein kinase bind in the ATP site. Journal of Biological Chemistry 1997;272:12116-21.
53. Kaiser RA, Lyons JM, Duffy JY, et al. Inhibition of p38 reduces myocardial infarction injury in the mouse but not pig after ischemia-reperfusion. American Journal of Physiology-Heart and Circulatory Physiology 2005;289:H2747-H2751.

54. Kaiser RA, Bueno OF, Lips DJ, et al. Targeted inhibition of p38 mitogen-activated protein kinase antagonizes cardiac injury and cell death following ischemia-reperfusion in vivo. Journal of Biological Chemistry 2004;279:15524-30.
55. See F, Thomas W, Way K, et al. p38 mitogen-activated protein kinase inhibition improves cardiac function and attenuates left ventricular remodeling following myocardial infarction in the rat. Journal of the American College of Cardiology 2004;44:1679-89.
56. Gerber HP, McMurtrey A, Kowalski J, et al. Vascular endothelial growth factor regulates endothelial cell survival through the phosphatidylinositol 3 '-kinase Akt signal transduction pathway - Requirement for Flk-1/KDR activation. Journal of Biological Chemistry 1998;273:30336-43.
57. Hausenloy DJ, Yellon DM. Cardioprotective growth factors. Cardiovasc Res 2009;83:179-94.
58. Meloni M, Caporali A, Graiani G, et al. Nerve Growth Factor Promotes Cardiac Repair following Myocardial Infarction. Circulation Research 2010;106:1275-U230.
59. Beltrami AP, Barlucchi L, Torella D, et al. Adult cardiac stem cells are multipotent and support myocardial regeneration. Cell 2003;114:763-76.
60. Cimini M, Fazel S, Zhuo S, et al. c-kit dysfunction impairs myocardial healing after infarction. Circulation 2007;116:I77-I82.
61. Xiang FL, Lu XR, Hammoud L, et al. Cardiomyocyte-Specific Overexpression of Human Stem Cell Factor Improves Cardiac Function and Survival After Myocardial Infarction in Mice. Circulation 2009;120:1065-U78.
62. Reichardt LF. Neuratrophin-regulated signalling pathways. Philosophical Transactions of the Royal Society B-Biological Sciences 2006;361:1545-64.
63. Caporali A, Emanueli C. Cardiovascular Actions of Neurotrophins. Physiological Reviews 2009;89:279-308.
64. Calissano P, Amadoro G, Matrone C, et al. Does the term 'trophic' actually mean anti-amyloidogenic? The case of NGF. Cell Death and Differentiation 2010;17:1126-33.
65. Chao MV, Rajagopal R, Lee FS. Neurotrophin signalling in health and disease. Clinical Science 2006;110:167-73.

66. Strande JL, Routhu KV, Lecht S, Lazarovici P. Nerve growth factor reduces myocardial ischemia/reperfusion injury in rat hearts. J Basic Clin Physiol Pharmacol 2013;24:81-4.
67. Liskamp RMJ, Rijkers DTS, Kruijtzer JAW, Kemmink J. Peptides and Proteins as a Continuing Exciting Source of Inspiration for Peptidomimetics. Chembiochem 2011;12:1626-53.
68. Scarpi D, Cirelli D, Matrone C, et al. Low molecular weight, non-peptidic agonists of TrkA receptor with NGF-mimetic activity. Cell Death & Disease 2012;3.
69. O'Neal WT, Griffin WF, Kent SD, Virag JAI. Cellular Pathways of Death and Survival in Acute Myocardial Infarction. J Clin Exp Cardiolog 2012.
70. Eltzschig HK, Eckle T. Ischemia and reperfusion-from mechanism to translation. Nature Medicine 2011;17:1391-401.
71. Abagyan R, Totrov M. Biased Probability Monte-Carlo Conformational Searches and Electrostatic Calculations for Peptides and Proteins. Journal of Molecular Biology 1994;235:983-1002.
72. An J, Totrov M, Abagyan R. Pocketome via comprehensive identification and classification of ligand binding envelopes. Mol Cell Proteomics 2005;4:752-61.
73. Michael LH, Entman ML, Hartley CJ, et al. Myocardial ischemia and reperfusion: A murine model. American Journal of Physiology-Heart and Circulatory Physiology 1995;269:H2147-H2154.
74. Sengupta A, Molkentin JD, Paik JH, et al. FoxO Transcription Factors Promote Cardiomyocyte Survival upon Induction of Oxidative Stress. Journal of Biological Chemistry 2011;286:7468-78.
75. Abas L, Bogoyevitch MA, Guppy M. Mitochondrial ATP production is necessary for activation of the extracellular-signal-regulated kinases during ischaemia/reperfusion in rat myocyte-derived H9c2 cells. Biochemical Journal 2000;349:119-26.
76. Ma LJ, Liu HM, Xie ZL, et al. Ginsenoside Rb3 Protects Cardiomyocytes against Ischemia-Reperfusion Injury via the Inhibition of JNK-Mediated NF-kappa B Pathway: A Mouse Cardiomyocyte Model. Plos One 2014;9.

77. Forsythe JA, Jiang BH, Iyer NV, et al. Activation of vascular endothelial growth factor gene transcription by hypoxia-inducible factor 1. Molecular and Cellular Biology 1996;16:4604-13.
78. Ahn A, Frishman WH, Gutwein A, et al. Therapeutic Angiogenesis A New Treatment Approach for Ischemic Heart Disease - Part I. Cardiology in Review 2008;16:163-71.
79. Takahashi N, Seko Y, Noiri E, et al. Vascular endothelial growth factor induces activation and subcellular translocation of focal adhesion kinase (p125(FAK)) in cultured rat cardiac myocytes. Circulation Research 1999;84:1194-202.
80. Kolk MV, Meyberg D, Deuse T, et al. LAD-ligation: a murine model of myocardial infarction. J Vis Exp 2009.